

doi: 10.17586/2226-1494-2025-25-3-457-465

Deep learning-enhanced contour interpolation techniques for 3D carotid vessel wall segmentation

Nouar Ismail¹, Alexandra S. Vatian², Tatyana A. Poleyaya³, Alexander A. Golubev⁴,
Dmitry A. Dobrenko⁵, Alexey A. Zubanenko⁶, Natalia F. Gusarova⁷✉, Almaz G. Vanyurkin⁸,
Mikhail A. Chernyavskiy⁹

^{1,2,3,4,5,6,7} ITMO University, Saint Petersburg, 197101, Russian Federation

⁶ IMV LLC, Saint Petersburg, 191119, Russian Federation

^{8,9} Almazov National Medical Research Centre, Saint Petersburg, 197341, Russian Federation

¹ noauresmail@gmail.com, <https://orcid.org/0009-0003-3545-9719>

² alexvatyan@gmail.com, <https://orcid.org/0000-0002-5483-716X>

³ tx15003@gmail.com, <https://orcid.org/0000-0001-6131-0019>

⁴ 9459539@gmail.com, <https://orcid.org/0000-0001-7417-6947>

⁵ enotpalaskun@gmail.com, <https://orcid.org/0009-0006-1485-1166>

⁶ zubdocmri@gmail.com, <https://orcid.org/0000-0001-6953-5239>

⁷ natfed@list.ru✉, <https://orcid.org/0000-0002-1361-6037>

⁸ almaz.vanyurkin@mail.ru, <https://orcid.org/0000-0002-8209-9993>

⁹ machern@mail.ru, <https://orcid.org/0000-0003-1214-0150>

Abstract

When studying human vessels using the contour interpolation method, there is a problem of insufficient data for training neural networks for automatic segmentation of the carotid artery wall. In this paper, automated methods of contour interpolation are proposed to expand the datasets, which allows for improved segmentation of vessel walls and atherosclerotic plaques. In this study, the performance of various interpolation methods is compared with the traditional nearest neighboring technique. A theoretical description and comparative evaluation of Linear, Polar, and Spline interpolation are presented. Quantitative metrics, including the Dice Similarity Coefficient, area and index differences, and normalized Hausdorff distances, are used to evaluate the performance of the methods. Performance evaluations are performed on various vessel morphologies for both the lumen and the outer wall boundaries. The study showed that Linear interpolation achieves better geometric performance (Cohen's Kappa 0.92) and improved neural network performance (Score 0.86) compared to the State-of-the-Art model. The proposed interpolation methods consistently outperform nearest neighbor interpolation. Polar and spline methods are effective in generating anatomically plausible contours with improved smoothness and continuity, eliminating transition artifacts between slices. Statistical analysis confirmed good agreement and reduced variation of these methods. The results of the study are useful for the development of automated tools for assessing atherosclerotic plaque in carotid arteries, which is important for stroke prevention. Implementation of improved interpolation methods into clinical imaging workflows can significantly improve the reliability, accuracy, and clinical utility of vessel wall segmentation.

Keywords

carotid vessel, wall segmentation, contour interpolation, deep learning, plaques, carotid atherosclerosis

Acknowledgements

This work was supported by the Russian Science Foundation, Grant No. 23-11-00346.

For citation: Ismail N., Vatian A.S., Poleyaya T.A., Golubev A.A., Dobrenko D.A., Zubanenko A.A., Gusarova N.F., Vanyurkin A.G., Chernyavskiy M.A. Deep learning-enhanced contour interpolation techniques for 3D carotid vessel wall segmentation. *Scientific and Technical Journal of Information Technologies, Mechanics and Optics*, 2025, vol. 25, no. 3, pp. 457–465. doi: 10.17586/2226-1494-2025-25-3-457-465

УДК 004.932

Методы интерполяции контуров с использованием глубокого обучения для трехмерной сегментации стенки сонных артерий

Нуар Исмаил¹, Александра Сергеевна Ватъян², Татьяна Андреевна Полевая³,
Александр Андреевич Голубев⁴, Дмитрий Александрович Добренко⁵,
Алексей Александрович Зубаненко⁶, Наталия Федоровна Гусарова⁷✉,
Алмаз Гафурович Ванюркин⁸, Михаил Александрович Чернявский⁹

^{1,2,3,4,5,6,7} Университет ИТМО, Санкт-Петербург, 197101, Российская Федерация

⁶ ООО ИМВИЖН, Санкт-Петербург, 191119, Российская Федерация

^{8,9} Национальный медицинский исследовательский центр имени В.А. Алмазова, Санкт-Петербург, 197341, Российская Федерация

¹ noauresmail@gmail.com, <https://orcid.org/0009-0003-3545-9719>

² alexvatyan@gmail.com, <https://orcid.org/0000-0002-5483-716X>

³ tx15003@gmail.com, <https://orcid.org/0000-0001-6131-0019>

⁴ 9459539@gmail.com, <https://orcid.org/0000-0001-7417-6947>

⁵ enotpalaskun@gmail.com, <https://orcid.org/0009-0006-1485-1166>

⁶ zubdocmri@gmail.com, <https://orcid.org/0000-0001-6953-5239>

⁷ natfed@list.ru✉, <https://orcid.org/0000-0002-1361-6037>

⁸almaz.vanyurkin@mail.ru, <https://orcid.org/0000-0002-8209-9993>

⁹ machern@mail.ru, <https://orcid.org/0000-0003-1214-0150>

Аннотация

Введение. При исследовании сосудов человека методом интерполяции контуров возникает проблема недостатка данных для обучения нейронных сетей с целью автоматической сегментации стенки сонной артерии. В работе предложены автоматизированные методы интерполяции контуров для расширения наборов данных, что позволяет улучшить сегментацию стенок сосудов и атеросклеротических бляшек. В представленном исследовании оценивается эффективность различных методов интерполяции в сравнении с традиционной техникой ближайшего соседа. **Методы.** Представлены теоретическое описание и сравнительная оценка линейной, полярной и сплайн-интерполяции. Для оценки производительности методов использованы количественные метрики, включая коэффициент сходства Дайса, различия в площади и индексе, а также нормализованные расстояния Хаусдорфа. Оценки производительности выполнены на различных морфологиях сосудов как для просвета, так и для внешних границ стенок. **Основные результаты.** Исследование показало, что линейная интерполяция достигает лучших геометрических показателей (Каппа Коэна 0,92) и улучшенной эффективности нейронной сети (оценка 0,86) по сравнению с передовой моделью. Предложенные методы интерполяции стабильно превосходят интерполяцию ближайшего соседа. Полярные и сплайн-методы эффективны при создании анатомически правдоподобных контуров с улучшенной гладкостью и непрерывностью, устраняют артефакты перехода между срезами. Статистический анализ подтвердил хорошую согласованность и уменьшение вариации этих методов. **Обсуждение.** Результаты исследования полезны для разработки автоматизированных инструментов оценки атеросклеротических бляшек в сонных артериях, что важно для профилактики инсульта. Внедрение улучшенных методов интерполяции в клинические рабочие процессы визуализации может значительно повысить надежность, точность и клиническую полезность сегментации стенок сосудов.

Ключевые слова

сонные артерии, сегментация стенки, интерполяция контура, глубокое обучение, бляшки, атеросклероз сонной артерии

Благодарности

Исследование поддержано грантом Российского научного фонда, № 23-11-00346.

Ссылка для цитирования: Исмаил Н., Ватъян А.С., Полевая Т.А., Голубев А.А., Добренко Д.А., Зубаненко А.А., Гусарова Н.Ф., Ванюркин А.Г., Чернявский М.А. Методы интерполяции контуров с использованием глубокого обучения для трехмерной сегментации стенки сонных артерий // Научно-технический вестник информационных технологий, механики и оптики. 2025. Т. 25, № 3. С. 457–465 (на англ. яз.). doi: 10.17586/2226-1494-2025-25-3-457-465

Introduction

Methods of Carotid Stenosis Imaging

Atherosclerosis is a leading cause of cardiovascular diseases, with plaque being built up within the arterial walls. The serious outcomes of this include stroke, heart attack, and peripheral artery disease. Of the various regions that are affected, carotid atherosclerosis refers to hardening and narrowing of carotid arteries, with a very high risk from its potential to cause ischemic strokes. The carotid arteries are the vessels through which oxygenated blood reaches the brain. Over time, plaques along their inner walls can

reduce or block blood flow. In worse conditions, plaques may break off and cause strokes. The prevalence of carotid atherosclerosis is high, especially in aging populations and individuals with comorbid conditions, such as hypertension, diabetes, and hyperlipidemia.

Detection and evaluation of the severity of carotid atherosclerosis can prevent catastrophic cardiovascular events. Traditionally, carotid ultrasound represented the first-line imaging modality for such studies, while Magnetic Resonance Imaging (MRI) represented a second-level method for the study of carotid stenosis [1]. However, in recent years, several 3D black-blood MR sequences

with high isotropic resolution, high signal-to-noise ratio, and large coverage have been developed [2, 3]. Among them, 3D-VISTA (Volume Isotropic Turbo Spin Echo Acquisition) method allows large coverage of carotid arteries with submillimeter isotropic resolution in the coronal acquisition, and can depict atherosclerotic lesion burden, severity, and luminal stenosis. This technique enables submillimeter isotropic resolution, allowing comprehensive visualization of the lumen and outer wall. However, challenges remain, including the complexity of 3D image review, large datasets, and the need for extensive training of radiologists to interpret vessel wall thickness accurately. These limitations underscore the importance of developing automated tools for segmentation and measurement of above-mentioned 3D-VISTA images.

Deep learning has emerged as a revolutionary technology in medical imaging. According to [4], Convolutional Neural Networks (CNNs) outperform traditional methods in a range of image segmentation tasks. Carotid atherosclerosis, requiring precise segmentation of the carotid artery, benefits greatly from these advancements. Accurate segmentation is critical for assessing plaque burden, measuring lumen diameter, and determining stenosis. Fig. 1 illustrates the segmentation process, highlighting lumen and arterial wall separation for measurements.

Due to the high potential of 3D-VISTA approach, a specialized Vessel Wall Segmentation Challenge 2022 was dedicated to it. Its primary task was to segment the carotid vessel wall from 3D-VISTA images, enabling clinically relevant measurements, such as wall thickness, lumen area, and stenosis percentage. Our work builds on these objectives by addressing the interpolation of missing annotations and enhancing the segmentation pipeline for robust and clinically applicable results.

Related Works

Several segmentations schemes have been developed over the years to increase accuracy. A semi-automatic

technique was developed in [5], who introduced an inner pathfinding algorithm with active contours without edges. This approach optimized the image-dependent force to detect the walls of the carotid artery, yielding highly accurate results with a Dice coefficient of 0.949. Another semi-automated methods utilized algorithms such as graph cuts and watershed [6]. However, these methods require significant user involvement, making them unsuitable for large-scale clinical settings.

Among the fully automated techniques, the first was the work [7] presenting a method for segmenting and labeling head and neck vessels from CTA volumes. Now among fully automated methods, deep learning-based ones [8–15] completely dominate. Authors [16] pioneered the use of U-Net for coronary artery segmentation and stenosis classification on CTA images. Their work demonstrated the power of CNNs in addressing anatomical variability, and plaque morphology—challenges also present in carotid artery segmentation. Their approach achieved a Dice score of 0.771 for segmentation and an accuracy of 0.750 for stenosis classification. The work [17] introduced a CNN-based approach reformulated as a multi-task regression in polar coordinates for black-blood MRI carotid artery segmentation, achieving a median Dice similarity coefficient of 0.813. Another notable method, CarotidNet [10], employed a 3D convolutional neural network with residual connections and dilated convolutions to segment the carotid artery bifurcation from CTA images, achieving a Dice similarity coefficient of 0.823.

Hybrid approaches have recently gained traction by integrating deep learning with traditional segmentation models. The work [18] proposed a shape-constrained active contour model initialized using deep learning outputs to segment the carotid artery lumen from MR images. This hybrid framework utilized a probability atlas for outer artery wall detection, achieving segmentation accuracy comparable to manual methods while reducing dependency on large labeled datasets. In [9] the Gated

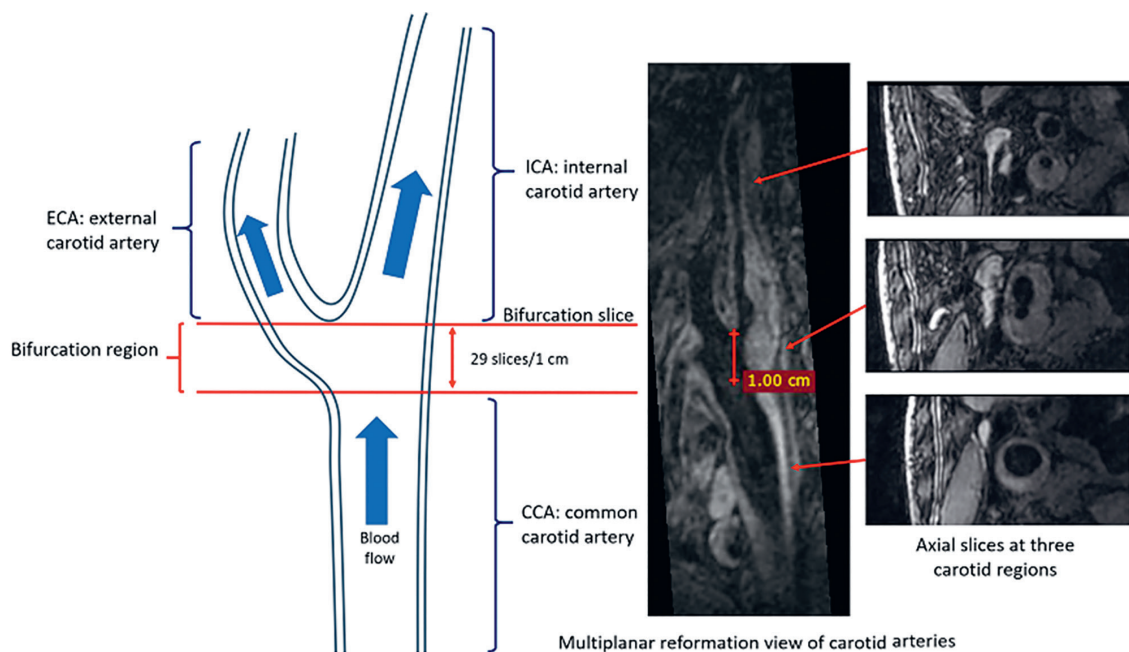


Fig. 1. Illustration of the carotid artery anatomy and corresponding 3D-VISTA images

Multi-Task Network (GMT-Net) is introduced which jointly performs lumen segmentation, outer wall segmentation, and carotid atherosclerosis diagnosis on black-blood MRI. By leveraging multi-task learning and novel gated exchange and fusion layers, the model effectively captured task correlations, achieving Dice scores of 0.9677 and 0.9669 for lumen and outer wall segmentation, respectively, and an AUC of 0.9516 for diagnosis accuracy on the CAREII dataset.

While highly effective, all the above methods rely on a large, annotated dataset, which is challenging in scaling them to smaller datasets. On the contrary, a few works focus on enhancing preprocessing techniques to improve label interpolation before deep learning model training. Specifically, [19] utilized a nearest-neighbor interpolation technique to address the challenge of missing annotations, effectively propagating labels across slices with sparse manual annotations. Notably, their approach achieved the first rank in the Vessel Wall Segmentation 2022 Challenge based on quantitative metrics, so we used it as State-of-the-Art (SOTA) model in our work. However, in our opinion, the potential of interpolation methods is not exhausted by this approach. To test this hypothesis, in our study, we applied three distinct interpolation techniques — Linear, Polar, and Spline interpolation — to generate intermediate contours between annotated slices in a 3D MRI dataset. These methods provided different approaches to interpolate contours based on specific mathematical principles, ensuring smooth transitions between contours in regions lacking direct annotations. The interpolated contours were then used as inputs to our segmentation pipeline to enhance the segmentation of lumen and outer wall structures. Additionally, the performance of these techniques was benchmarked by evaluating their impact on segmentation accuracy, plaque detection, and vessel wall measurement, highlighting their contribution to addressing the challenge of unannotated slices.

Experiments Methodology

Dataset

The dataset used in this study is the Carotid Artery Vessel Wall Segmentation Challenge 2022 dataset consisting images of the carotid artery formed using 3D-VISTA approach. It has specifically been designed for the automation of vessel wall segmentation and has intensive segmentation for both lumen and outer wall in the carotid artery. It provides high resolution images of internal, external, and common carotid arteries, as illustrated in Fig. 1, enabling accurate segmentation, plaque detection, and measurement of vessel wall thickness, all essential for the diagnosis and risk assessment of atherosclerosis.

Each case consists of an axial resliced 3D image volume, with typical dimensions of height 100 px, width 432 px, and depth 432 slices. However, only the middle slices were considered for the assessment of the vessel wall due to the appropriate coronary scan technique. Of these, 80 % of such slices were unannotated and required interpolation techniques to deal with the nonavailability of annotation data. The total dataset includes 50 training cases comprising 2584 manually annotated slices of both

left and right carotids, which outline the contours of the vessel walls: internal common carotid as well as the external carotid. However, due to variable image quality in this dataset, only slices where the vessel wall is clearly visible have been annotated. These annotations originated using the CASCADE software, renowned for its sub-pixel accuracy in vessel wall delineation.

The dataset was annotated in an XML format, using the CASCADE software/algorithm, demonstrate high-resolution visualization of the vessel wall, aiding in the segmentation of lumen and outer wall structures. For the evaluation of participants, key metrics included the Dice Similarity Coefficient (DSC), Hausdorff Distance (HD), and lumen and wall area differences to assess anatomic accuracy and ensure clinically usable results from segmentations. The DSC, defined as

$$DSC = \frac{2|A \cap B|}{|A| + |B|}$$

measures the overlap between the predicted segmentation A and ground truth B . The HD, calculated as

$$HD(A, B) = \max(\sup_{a \in A} \inf_{b \in B} d(a, b), \sup_{b \in B} \inf_{a \in A} d(a, b)),$$

quantifies the largest boundary distance between A and B . Cohen's kappa metric, defined as

$$\kappa = \frac{p_0 - p_e}{1 - p_e},$$

where p_0 represents the observed agreement and p_e the expected agreement by chance, was used to evaluate the inter-rater or algorithmic reliability of segmentation annotations. The normalized area difference was determined using

$$\Delta Area = \frac{|A_{predicted} - A_{GroundTruth}|}{A_{GroundTruth}}$$

providing insights into the clinical relevance of segmentation accuracy.

Preprocessing

Preprocessing is a very significant step in medical image analysis, predominantly when there is incomplete full annotation of the dataset. Only 20 % of slices were manually annotated in the dataset that had been used for this study. To address the lack of annotated slices in the dataset, interpolation techniques were employed to propagate the lumen and wall annotations to unannotated slices. As shown in Fig. 2, the segmentation process involves identifying the lumen and subsequently annotating the outer wall of the carotid artery.

The vessel walls were divided into two important categories to address the discontinuity in the annotations: normal vessel walls and atherosclerotic vessel walls. These differentiation aspects are crucial because variations in the anatomy and pathology can significantly affect the accuracy of segmentation models. Additionally, lumen areas were labeled separately to ensure the accurate representation of vessel structure at a particular point, which is critical for diagnosing stenosis and assessing overall vessel health.

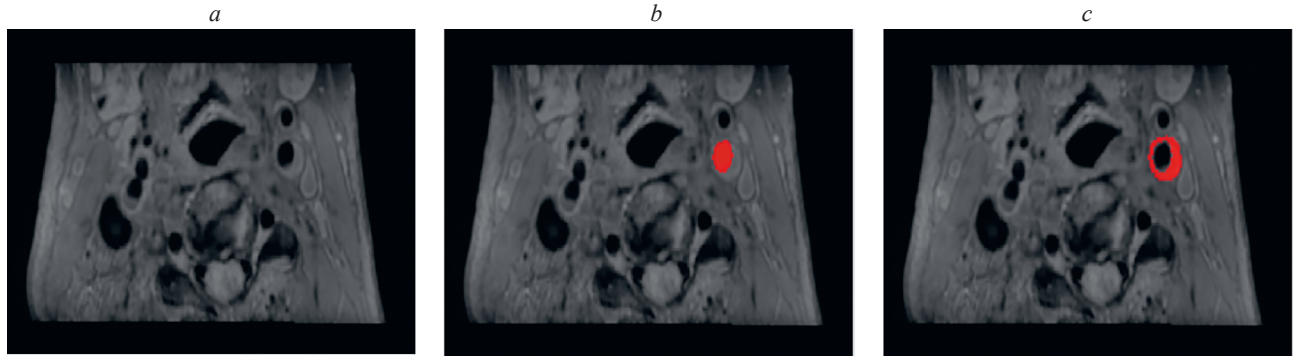


Fig. 2. Visualization of the annotation process for carotid artery segmentation: original axial MRI slice (a); lumen segmentation (b); lumen and outer wall segmentation (c)

Interpolation Methods

Linear Interpolation. Linear interpolation is the most straightforward technique where each point on the interpolated contour is computed as a weighted average between corresponding points on two adjacent contours. Given two contours at slices z_0 and z_1 with points P_0 and P_1 , the linearly interpolated contour at an intermediate slice z_t is given by:

$$P_t = (1 - t)P_0 + tP_1,$$

where t is the normalized interpolation parameter, $0 \leq t \leq 1$. This method provides a direct interpolation of the positions of points but can produce unnatural shapes if the contours are highly irregular, as it does not account for radial transformations or curvature.

Polar Interpolation. Polar interpolation is a modification of Linear interpolation that operates in polar coordinates relative to a centroid, making it more suitable for shapes with rotational symmetry or roughly circular geometry. First, the centroid of each contour is calculated. Then, the contour points are converted to polar coordinates, yielding radius r and angle θ for each point. For corresponding points on two contours, the interpolated radius r_t at an intermediate slice is calculated as:

$$r_t = (1 - t)r_0 + tr_1,$$

while keeping the angle θ constant. The interpolated points are then converted back to Cartesian coordinates. This approach helps maintain the radial structure of the contours, reducing distortions that can arise with linear interpolation when working with circular or elliptical shapes.

Spline Interpolation. To achieve smoother interpolations, we employed Spline interpolation, specifically B-splines, which provide a continuous and smooth fit to the contour points by using piecewise polynomial functions. B-splines are defined by a set of control points and a degree (or order) κ of the polynomial, which determines the smoothness and flexibility of the spline. In our implementation, we selected control points from each original contour and constructed a spline for both x and y coordinates separately.

Let $P_i = (x_i, y_i)_{i=1}^n$ be the set of n points on a given contour. A B-spline $S(t)$ for each coordinate is defined as a weighted sum of basis functions $N_{i,\kappa}(t)$:

$$S_x(t) = \sum_{i=1}^n x_i N_{i,\kappa}(t), S_y(t) = \sum_{i=1}^n y_i N_{i,\kappa}(t),$$

where t is a parameter (typically normalized to range from 0 to 1), and $N_{i,\kappa}(t)$ are the B-spline basis functions of degree κ . The basis functions are recursively defined, starting from $\kappa = 0$ as:

$$N_{i,0}(t) = \begin{cases} 1, & \text{if } t_i \leq (t) < t_{i+1}, \\ 0, & \text{otherwise,} \end{cases}$$

where $\{t_i\}$ is the knot vector that defines the intervals over which each basis function is non-zero.

For a pair of contours on slices z_0 and z_1 , we construct B-splines $S_{x,z_0}(t)$, $S_{y,z_0}(t)$ and $S_{x,z_1}(t)$, $S_{y,z_1}(t)$ for each contour. To interpolate a contour for an intermediate slice z_t (where t is between 0 and 1), we calculate intermediate splines $S_{x,t}(t)$ and $S_{y,t}(t)$ as:

$$S_{x,t}(t) = (1 - t)S_{x,z_0}(t) + tS_{x,z_1}(t),$$

$$S_{y,t}(t) = (1 - t)S_{y,z_0}(t) + tS_{y,z_1}(t).$$

The interpolated contour points for slice z_t are then given by evaluating $S_{x,t}(t)$ and $S_{y,t}(t)$ at uniformly spaced values of t (e.g., from 0 to 1 in equal intervals to ensure uniform sampling).

This approach allows each interpolated contour to inherit the smoothness of the original B-spline functions, providing a natural and continuous shape. The piecewise polynomial nature of B-splines ensures that any sharp changes or high curvature present in the original contours are appropriately captured, while avoiding artifacts like abrupt angles or linear segments that may appear with simpler interpolation methods.

The overall framework implementation for carotid artery segmentation, from preprocessing to final model training, is illustrated in Fig. 3. This pipeline includes preprocessing and label splitting, followed by contours interpolation, machine learning-based label propagation, and the final nnUNet model training.

nnUNet Model Training

After pre-processing, the full image volumes of segmentation results were trained and predicted using the nnUNet model. nnUNet is one of the most important frameworks in medical image segmentation due to its capability in adapting model architecture and hyper

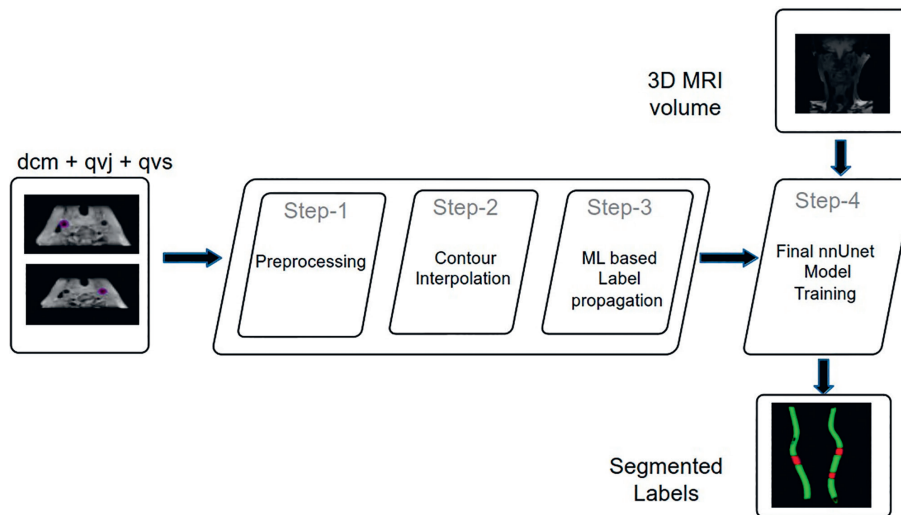


Fig. 3. Implementation of Carotid Artery Segmentation Framework: dcm — input DICOM file, qvj + qvs are XML files holding information about the annotations

parameters to the specifics of a given dataset with minimal manual tuning. Its strength lies in being self-configuring, thereby auto-tuning model settings for image modalities, resolutions, and segmentation tasks across medical datasets.

In our approach, we first trained the nnUNet on the interpolated labels from preprocessing. Training was done on fully interpolated labels throughout the volume of the 3D image, allowing the network to learn from both slices with and without annotations. Segmentation of medical imagery, including this dataset, highlights the strengths of nnUNet. It demonstrates resilience with respect to complex anatomical structures, such as the shapes of the carotid artery wall and the potential presence of atherosclerotic plaques.

The final model used was the nnUNetV2 version which includes several improvements related to efficiency, increasing image sizes, and integrating recent innovations in medical image segmentation. Generally, nnUNet generalizes well to various datasets and medical imaging modalities, making it particularly well-suited for use cases with only a few annotations available in the dataset. By combining both automatic configuration and robust architectural features, the nnUNet model has become the SOTA solution in medical image segmentation, ranking first consecutively in competitions like MICCAI.

The combination of contours interpolation during pre-processing with the powerful architecture of nnUNet created an effective pipeline for segmenting vessel walls of the carotid artery, even with only partial annotations. This approach ensured robust and accurate segmentation, addressing challenges of incomplete labeling and the complex anatomical structures encountered in medical imaging.

Experiments and Results

Implementation Details and Evaluation Metric

The available dataset, consisting of 50 cases, was divided into a training set and a testing set. Specifically, 43 cases (cases 3 to 7, 15, and 17 to 54) were designated for training, while 7 cases (cases 8 to 14) were reserved for testing.

The model was trained for 500 epochs without employing cross-validation to evaluate its performance on the test set.

For this implementation, we utilized an NVIDIA RTX 4060 GPU. It is important to note that all data augmentation techniques, such as random cropping, random rotation, random scaling, random flipping, random Gaussian noise addition, and elastic deformation, were automatically handled by the nnUNet framework. These augmentation techniques were applied by the model to increase the diversity of the training data without any manual intervention.

Results

In this study, we evaluated four interpolation methods — Linear, Nearest Neighbor, Polar, and Spline interpolation — on cases 8, 9, 10, 11, 12, 13, and 14. Our results were then compared with those from the official challenge page of the Vessel Wall Segmentation Challenge 2022, where models were trained on a more extensive dataset (50 cases) and evaluated on a larger test set (25 cases) compared to our limited dataset (43 training cases and 7 test cases). These results were used as SOTA model. Additionally, our requests to obtain annotated test cases from the challenge organizers went unanswered, limiting our ability to directly validate against the challenge data.

The results are presented in Table.

Among the four interpolation methods tested, Polar interpolation generally performed well across most metrics, balancing accuracy and computational stability, particularly in cases with few missing slices. The Spline interpolation method, however, showed high variability, especially in more complex cases with irregular contours, as evidenced by its DSC, lumen area, and wall area differences. For example, case 11 displayed substantial anomalies across all interpolation methods, with Polar and Spline interpolations yielding particularly high errors in Hausdorff Distance and Normalized Wall Index Difference. The inconsistency in case 11 could be attributed to significant structural differences or abnormalities in the vessel wall contours, causing instability in interpolation-based reconstructions. Notably, similar anomalies were detected when applying

Table. Comparison of Contour Interpolation Techniques Results for Carotid Vessel Wall Segmentation Metrics

Metrics	Interpolation Methods			
	Linear	Spline	Polar	SOTA
DSC	0.80	0.72	0.76	0.73
Lumen Area Difference	0.07	0.05	0.06	0.08
Wall Area Difference	0.09	0.18	0.13	0.18
Normalized Wall Index Difference	0.79	3.74	1.01	2.64
Hausdorff Distance (Lumen)	0.17	0.16	0.16	0.17
Hausdorff Distance (Wall)	0.38	0.98	0.58	1.16
Cohen's Kappa	0.92	0.64	0.77	0.85
Quantitative Score	0.86	0.75	0.80	0.79

the Nearest Neighbor interpolation method, indicating that these variances might be inherent to the data or an indication of irregular anatomy in these cases.

Comparing Linear interpolation to Nearest Neighbor interpolation, we found that Linear interpolation yielded consistently higher Quantitative Scores and lower wall area differences, indicating its better ability to smooth transitions between slices. Nearest Neighbor interpolation, however, provided competitive results in lumen area differences and sometimes surpassed Linear in Cohen's Kappa, suggesting that it may better preserve abrupt contour changes in cases with more regular slice structures.

Overall, the Polar interpolation method emerges as a balanced choice, particularly when maintaining smoothness between slices is crucial. Linear interpolation also remains a solid choice for cases with relatively even contours, while Spline interpolation high sensitivity to contour irregularities makes it less reliable in structurally complex cases.

Conclusion

In conclusion, the analysis and comparison of different contour interpolation methods, namely Polar interpolation,

Spline interpolation, and Linear interpolation, demonstrated superior performance over the nearest-neighbor interpolation method across several key evaluation metrics. The suggested interpolation methods consistently yielded higher Dice Similarity Coefficient scores, reduced area and index differences, and smaller normalized Hausdorff distances for both lumen and wall boundaries. These improvements indicate more precise and reliable segmentation, especially in cases where slice alignment is challenging. The enhanced performance of Polar and Spline interpolation methods over nearest-neighbor interpolation is evident in their ability to produce smoother and more anatomically accurate contours, reducing abrupt transitions between slices. This accuracy is particularly beneficial in clinical applications where precise wall and lumen boundaries are essential for diagnostics and treatment planning. The statistical analysis further supports the consistency and robustness of the proposed interpolation techniques, with reduced variance in the results compared to nearest-neighbor interpolation. Therefore, these advanced contour interpolation methods present a valuable improvement for vessel wall segmentation, offering greater accuracy and dependability in medical imaging workflows.

References

- David E., Grazhdani H., Aliotta L., Gavazzi L.M., Foti P.V., Palmucci S., Ini C., Tiralongo F., Castiglione D., Renda M., Pacini P., Di Bella C., Solito C., Gigli S., Fazio A., Bella R., Basile A., Cantisani V. Imaging of carotid stenosis: where are we standing? Comparison of multiparametric ultrasound, CT angiography, and MRI angiography, with recent developments. *Diagnostics*, 2024, vol. 14, no. 16, pp. 1708. <https://doi.org/10.3390/diagnostics14161708>
- Wei H., Zhang M., Li Y., Zhao X., Canton G., Sun J., Xu D., Zhou Z., Chen S., Ferguson M., Hatsukami T., Li R., Yuan C. Evaluation of 3D multi-contrast carotid vessel wall MRI: a comparative study. *Quantitative Imaging in Medicine and Surgery*, 2020, vol. 10, no. 1, pp. 269–282. <https://doi.org/10.21037/qims.2019.09.11>
- Deng F., Le L., Sharma R., et al. MR vessel wall imaging. Reference article. *Radiopaedia.org*. 2019. Available at: <https://doi.org/10.53347/rID-72016> (accessed: 24.01.2025)
- Litjens G., Kooi T., Beijndorf B.E., Setio A.A.A., Ciompi F., Ghafoorian M., van der Laak J.A.W.M., van Ginneken B., Sánchez C.I. A survey on deep learning in medical image analysis. *Medical Image Analysis*, 2017, vol. 42, pp. 60–88. <https://doi.org/10.1016/j.media.2017.07.005>
- Hachaj T., Ogiela M.R. Evaluation of carotid artery segmentation with centerline detection and active contours without edges algorithm. *Lecture Notes in Computer Science*, 2012, vol. 7465, pp. 468–478. https://doi.org/10.1007/978-3-642-32498-7_35

Литература

- David E., Grazhdani H., Aliotta L., Gavazzi L.M., Foti P.V., Palmucci S., Ini C., Tiralongo F., Castiglione D., Renda M., Pacini P., Di Bella C., Solito C., Gigli S., Fazio A., Bella R., Basile A., Cantisani V. Imaging of carotid stenosis: where are we standing? Comparison of multiparametric ultrasound, CT angiography, and MRI angiography, with recent developments // *Diagnostics*. 2024. V. 14. N 16. P. 1708. <https://doi.org/10.3390/diagnostics14161708>
- Wei H., Zhang M., Li Y., Zhao X., Canton G., Sun J., Xu D., Zhou Z., Chen S., Ferguson M., Hatsukami T., Li R., Yuan C. Evaluation of 3D multi-contrast carotid vessel wall MRI: a comparative study // *Quantitative Imaging in Medicine and Surgery*. 2020. V. 10. N 1. P. 269–282. <https://doi.org/10.21037/qims.2019.09.11>
- Deng F., Le L., Sharma R., et al. MR vessel wall imaging. Reference article // *Radiopaedia.org*. 2019 [Электронный ресурс]. URL: <https://doi.org/10.53347/rID-72016> (дата обращения: 24.01.2025)
- Litjens G., Kooi T., Beijndorf B.E., Setio A.A.A., Ciompi F., Ghafoorian M., van der Laak J.A.W.M., van Ginneken B., Sánchez C.I. A survey on deep learning in medical image analysis // *Medical Image Analysis*. 2017. V. 42. P. 60–88. <https://doi.org/10.1016/j.media.2017.07.005>
- Hachaj T., Ogiela M.R. Evaluation of carotid artery segmentation with centerline detection and active contours without edges algorithm // *Lecture Notes in Computer Science*. 2012. V. 7465. P. 468–478. https://doi.org/10.1007/978-3-642-32498-7_35

6. Hemmati H.R., Alizadeh M., Kamali-Asl A., Shirani S. Semi-automated carotid lumen segmentation in computed tomography angiography images. *Journal of Biomedical Research*, 2017, vol. 31, no. 6, pp. 548–558. <https://doi.org/10.7555/JBR.31.20160107>
7. Cuisenaire O. Fully automated carotid artery segmentation from CTA. *The MIDAS Journal*, 2009. <https://doi.org/10.54294/6mmv98>
8. Saba L., Sanagala S.S., Gupta S.K., Koppula V.K., Laird J.R., Viswanathan V., Sanches M.J., Kitas G.D., Johri A.M., Sharma N., Nicolaidis A., Suri J.S. A multicenter study on carotid ultrasound plaque tissue characterization and classification using six deep artificial intelligence models: A stroke application. *IEEE Transactions on Instrumentation and Measurement*, 2021, vol. 70, pp. 2505312. <https://doi.org/10.1109/TIM.2021.3052577>
9. Wu J., Xin J., Yang X., Matkovic L., Zhao X., Zheng N., Li R. Segmentation of carotid artery vessel wall and diagnosis of carotid atherosclerosis on black blood magnetic resonance imaging with multi-task learning. *Medical Physics*, 2023, vol. 51, no. 3, pp. 1775–1797. <https://doi.org/10.1002/mp.16728>
10. Zhou T., Tan T., Pan X., Tang H., Li J. Fully automatic deep learning trained on limited data for carotid artery segmentation from large image volumes. *Quantitative Imaging in Medicine and Surgery*, 2021, vol. 11, no. 1, pp. 67–83, 2021. <https://doi.org/10.21037/qims-20-286>
11. Samber D.D., Ramachandran S., Sahota A., Naidu S., Pruzan A., Fayad Z.A., Mani V. Segmentation of carotid arterial walls using neural networks. *World Journal of Radiol.*, 2020, vol. 12, no. 1, pp. 1–9. <https://doi.org/10.4329/wjr.v12.i1.1>
12. Wang J., Yu F., Zhang M., Lu J., Qian Z. A 3D framework for segmentation of carotid artery vessel wall and identification of plaque compositions in multi-sequence MR images. *Computerized Medical Imaging and Graphics*, 2024, vol. 116, pp. 102402. <https://doi.org/10.1016/j.compmedimag.2024.102402>
13. Huang Q., Tian H., Jia L., Li Z., Zhou Z. A review of deep learning segmentation methods for carotid artery ultrasound images. *Neurocomputing*. 2023. V. 545. P. 126298. <https://doi.org/10.1016/j.neucom.2023.126298>
14. Yoo SW., Yang S., Kim J., Huh K., Lee S., Heo M., Yi W. CACSNet for automatic robust classification and segmentation of carotid artery calcification on panoramic radiographs using a cascaded deep learning network. *Scientific Reports*, 2024, vol. 14, no. 1, pp. 13894. <https://doi.org/10.1038/s41598-024-64265-4>
15. Wang Y., Yao Y. Application of artificial intelligence methods in carotid artery segmentation: a review. *IEEE Access*, 2023, vol. 11, pp. 13846–13858. <https://doi.org/10.1109/ACCESS.2023.3243162>
16. Li Y., Wu Y., He J., Jiang W., Wang J., Peng Y., Jia Y., Xiong T., Jia K., Yi Z., Chen M. Automatic coronary artery segmentation and diagnosis of stenosis by deep learning based on computed tomographic coronary angiography. *European Radiology*, 2022, vol. 32, no. 9, pp. 6037–6045. <https://doi.org/10.1007/s00330-022-08761-z>
17. Alblas D., Brune C., Wolterink J.M. Deep learning-based carotid artery vessel wall segmentation in black-blood mri using anatomical priors. *Proceedings of SPIE*, 2022, vol. 12032, pp. 120320Y. <https://doi.org/10.1117/12.2611112>
18. Huang X., Wang J., Li Z. 3D carotid artery segmentation using shape-constrained active contours. *Computers in Biology and Medicine*, 2023, vol. 153, pp. 106530. <https://doi.org/10.1016/j.compbiomed.2022.106530>
19. Hu S., Liao Z., Xia Y. Label propagation for 3D carotid vessel wall segmentation and atherosclerosis diagnosis. *arXiv*, 2022, arXiv:2208.13337. <https://doi.org/10.48550/arXiv.2208.13337>
6. Hemmati H.R., Alizadeh M., Kamali-Asl A., Shirani S. Semi-automated carotid lumen segmentation in computed tomography angiography images // *Journal of Biomedical Research*. 2017. V. 31. N 6. P. 548–558. <https://doi.org/10.7555/JBR.31.20160107>
7. Cuisenaire O. Fully automated carotid artery segmentation from CTA // *The MIDAS Journal*. 2009. <https://doi.org/10.54294/6mmv98>
8. Saba L., Sanagala S.S., Gupta S.K., Koppula V.K., Laird J.R., Viswanathan V., Sanches M.J., Kitas G.D., Johri A.M., Sharma N., Nicolaidis A., Suri J.S. A multicenter study on carotid ultrasound plaque tissue characterization and classification using six deep artificial intelligence models: A stroke application // *IEEE Transactions on Instrumentation and Measurement*. 2021. V. 70. P. 2505312. <https://doi.org/10.1109/TIM.2021.3052577>
9. Wu J., Xin J., Yang X., Matkovic L., Zhao X., Zheng N., Li R. Segmentation of carotid artery vessel wall and diagnosis of carotid atherosclerosis on black blood magnetic resonance imaging with multi-task learning // *Medical Physics*. 2023. V. 51. N 3. P. 1775–1797. <https://doi.org/10.1002/mp.16728>
10. Zhou T., Tan T., Pan X., Tang H., Li J. Fully automatic deep learning trained on limited data for carotid artery segmentation from large image volumes // *Quantitative Imaging in Medicine and Surgery*. 2021. V. 11. N 1. P. 67–83, 2021. <https://doi.org/10.21037/qims-20-286>
11. Samber D.D., Ramachandran S., Sahota A., Naidu S., Pruzan A., Fayad Z.A., Mani V. Segmentation of carotid arterial walls using neural networks // *World Journal of Radiol.* 2020. V. 12. N 1. P. 1–9. <https://doi.org/10.4329/wjr.v12.i1.1>
12. Wang J., Yu F., Zhang M., Lu J., Qian Z. A 3D framework for segmentation of carotid artery vessel wall and identification of plaque compositions in multi-sequence MR images // *Computerized Medical Imaging and Graphics*. 2024. V. 116. P. 102402. <https://doi.org/10.1016/j.compmedimag.2024.102402>
13. Huang Q., Tian H., Jia L., Li Z., Zhou Z. A review of deep learning segmentation methods for carotid artery ultrasound images // *Neurocomputing*. 2023. V. 545. P. 126298. <https://doi.org/10.1016/j.neucom.2023.126298>
14. Yoo SW., Yang S., Kim J., Huh K., Lee S., Heo M., Yi W. CACSNet for automatic robust classification and segmentation of carotid artery calcification on panoramic radiographs using a cascaded deep learning network // *Scientific Reports*. 2024. V. 14. N 1. P. 13894. <https://doi.org/10.1038/s41598-024-64265-4>
15. Wang Y., Yao Y. Application of artificial intelligence methods in carotid artery segmentation: a review // *IEEE Access*. 2023. V. 11. P. 13846–13858. <https://doi.org/10.1109/ACCESS.2023.3243162>
16. Li Y., Wu Y., He J., Jiang W., Wang J., Peng Y., Jia Y., Xiong T., Jia K., Yi Z., Chen M. Automatic coronary artery segmentation and diagnosis of stenosis by deep learning based on computed tomographic coronary angiography // *European Radiology*. 2022. V. 32. N 9. P. 6037–6045. <https://doi.org/10.1007/s00330-022-08761-z>
17. Alblas D., Brune C., Wolterink J.M. Deep learning-based carotid artery vessel wall segmentation in black-blood mri using anatomical priors // *Proceedings of SPIE*. 2022. V. 12032. P. 120320Y. <https://doi.org/10.1117/12.2611112>
18. Huang X., Wang J., Li Z. 3D carotid artery segmentation using shape-constrained active contours // *Computers in Biology and Medicine*. 2023. V. 153. P. 106530. <https://doi.org/10.1016/j.compbiomed.2022.106530>
19. Hu S., Liao Z., Xia Y. Label propagation for 3D carotid vessel wall segmentation and atherosclerosis diagnosis // *arXiv*. 2022. arXiv:2208.13337. <https://doi.org/10.48550/arXiv.2208.13337>

Authors

Nouar Ismail — PhD Student, ITMO University, Saint Petersburg, 197101, Russian Federation, <https://orcid.org/0009-0003-3545-9719>, noauresmail@gmail.com

Alexandra S. Vatian — PhD, Dean, ITMO University, Saint Petersburg, 197101, Russian Federation, <https://orcid.org/0000-0002-5483-716X>, alexvatyan@gmail.com

Tatyana A. Polevaya — Engineer, Software Developer, ITMO University, Saint Petersburg, 197101, Russian Federation, <https://orcid.org/0000-0001-6131-0019>, tx15003@gmail.com

Авторы

Исмаил Нуар — аспирант, Университет ИТМО, Санкт-Петербург, 197101, Российская Федерация, <https://orcid.org/0009-0003-3545-9719>, noauresmail@gmail.com

Ватьян Александра Сергеевна — кандидат технических наук, декан, Университет ИТМО, Санкт-Петербург, 197101, Российская Федерация, <https://orcid.org/0000-0002-5483-716X>, alexvatyan@gmail.com

Полевая Татьяна Андреевна — инженер, программист, Университет ИТМО, Санкт-Петербург, 197101, Российская Федерация, <https://orcid.org/0000-0001-6131-0019>, tx15003@gmail.com

Alexander A. Golubev — PhD Student, ITMO University, Saint Petersburg, 197101, Russian Federation, <https://orcid.org/0000-0001-7417-6947>, 9459539@gmail.com

Dmitry A. Dobrenko — PhD Student, ITMO University, Saint Petersburg, 197101, Russian Federation, [sc 58793748800](https://orcid.org/0009-0006-1485-1166), <https://orcid.org/0009-0006-1485-1166>, enotpalaskun@gmail.com

Alexey A. Zubanenko — CEO, IMV LLC, Saint Petersburg, 191119, Russian Federation; ITMO University, Saint Petersburg, 197101, Russian Federation; PhD Student, [sc 57215436184](https://orcid.org/0000-0001-6953-5239), <https://orcid.org/0000-0001-6953-5239>, zubdocmri@gmail.com

Natalia F. Gusarova — PhD, Senior Researcher, Associate Professor, ITMO University, Saint Petersburg, 197101, Russian Federation, [sc 57162764200](https://orcid.org/0000-0002-1361-6037), <https://orcid.org/0000-0002-1361-6037>, natfed@list.ru

Almaz G. Vanyurkin — Junior Researcher, Almazov National Medical Research Centre, Saint Petersburg, 197341, Russian Federation, [sc 57295278200](https://orcid.org/0000-0002-8209-9993), <https://orcid.org/0000-0002-8209-9993>, almaz.vanyurkin@mail.ru

Mikhail A. Chernyavskiy — D.Sc. (Medicine), Head of the Department of vascular and endovascular surgery, Almazov National Medical Research Centre, Saint Petersburg, 197341, Russian Federation, [sc 55840916800](https://orcid.org/0000-0003-1214-0150), <https://orcid.org/0000-0003-1214-0150>, machern@mail.ru

Голубев Александр Андреевич — аспирант, Университет ИТМО, Санкт-Петербург, 197101, Российская Федерация, <https://orcid.org/0000-0001-7417-6947>, 9459539@gmail.com

Добренко Дмитрий Александрович — аспирант, Университет ИТМО, Санкт-Петербург, 197101, Российская Федерация, [sc 58793748800](https://orcid.org/0009-0006-1485-1166), <https://orcid.org/0009-0006-1485-1166>, enotpalaskun@gmail.com

Зубаненко Алексей Александрович — генеральный директор, ООО ИМВИЖН, Санкт-Петербург, 191119, Российская Федерация; аспирант, Университет ИТМО, Санкт-Петербург, 197101, Российская Федерация, [sc 57215436184](https://orcid.org/0000-0001-6953-5239), <https://orcid.org/0000-0001-6953-5239>, zubdocmri@gmail.com

Гусарова Наталия Федоровна — кандидат технических наук, старший научный сотрудник, доцент, Университет ИТМО, Санкт-Петербург, 197101, Российская Федерация, [sc 57162764200](https://orcid.org/0000-0002-1361-6037), <https://orcid.org/0000-0002-1361-6037>, natfed@list.ru

Ванюркин Алмаз Гафурович — младший научный сотрудник, Национальный медицинский исследовательский центр имени В.А. Алмазова, Санкт-Петербург, 197341, Российская Федерация, [sc 57295278200](https://orcid.org/0000-0002-8209-9993), <https://orcid.org/0000-0002-8209-9993>, almaz.vanyurkin@mail.ru

Чернявский Михаил Александрович — доктор медицинских наук, заведующий НИО сосудистой и интервенционной хирургии, Национальный медицинский исследовательский центр имени В.А. Алмазова, Санкт-Петербург, 197341, Российская Федерация, [sc 55840916800](https://orcid.org/0000-0003-1214-0150), <https://orcid.org/0000-0003-1214-0150>, machern@mail.ru

Received 12.12.2024

Approved after reviewing 16.04.2025

Accepted 23.05.2025

Статья поступила в редакцию 12.12.2024

Одобрена после рецензирования 16.04.2025

Принята к печати 23.05.2025



Работа доступна по лицензии
Creative Commons
«Attribution-NonCommercial»